Nuclear Engineering and Technology 55 (2023) 4120–4124

Contents lists available at ScienceDirect

Nuclear Engineering and Technology

journal homepage: www.elsevier.com/locate/net

Original Article

The influence of air gaps on buffer temperature within an engineered barrier system

Seok Yoon *, Gi-Jun Lee

Disposal Safety Evaluation Research Division, Korea Atomic Energy Research Institute, Daejeon, 34057, Republic of Korea

ARTICLE INFO

Keywords:
Engineered barrier system
Gap space
Buffer temperature

ABSTRACT

High-level radioactive waste produced by nuclear power plants are disposed subterraneously utilizing an engineered barrier system (EBS). A gap inevitably exists between the disposal canisters and buffer materials, which may have a negative effect on the thermal transfer and water-blocking efficiency of the system. As few previous experimental works have quantified this effect, this study aimed to create an experimental model for investigating differences in the temperature changes of bentonite buffer in the presence and absence of air gaps between it and a surrounding stainless steel cell. Three test scenarios comprised an empty cell and cells partially or completely filled with bentonite. The temperature was measured inside the buffers and on the inner surface of their surrounding cells, which were artificially heated. The time required for the entire system to reach 100 °C was approximately 40% faster with no gap between the inner cell surface and the bentonite. This suggests that rock–buffer spaces should be filled in practice to ensure the rapid dissipation of heat from the buffer materials to their surroundings. However, it can be advantageous to retain buffer–canister gaps to lower the peak buffer temperature.

1. Introduction

It is necessary to safely dispose of high-level radioactive waste produced by nuclear power plants in rock layers several hundreds of meters below the Earth's surface, as such radioactive waste products are hazardous to humans [1,2]. Both natural and engineered barrier systems are utilized for the safe disposal of high-level radioactive waste. The KBS-3 disposal method developed by SKB and Posiva [3] involves the establishment of artificial barriers that consist of disposal canisters, bentonite buffer materials, and backfill materials that are installed in deposition holes which are drilled vertically into disposal tunnel floors, as shown in Fig. 1. After the installation of a disposal canister, its deposition hole will be filled with bentonite buffer; however, gaps inevitably form between the canister and the bentonite buffer blocks, as well as between the bentonite and the surrounding rock. This process is nevertheless used because it is easier to install bentonite buffer and backfill material, and, in the case of deposition holes with uneven rock walls, it is necessary to have regular spaces [4]. Countries at the forefront of radioactive waste disposal, such as Sweden and Finland, only permit canister–buffer gaps of up to 10 mm and rock–buffer gaps of up to 50 mm; in addition, the canister–buffer gaps are not filled, whereas the rock–buffer gaps are filled with smaller materials such as bentonite pellets or granules [4,6]. Such gaps need to be filled with materials, as they can cause disposal hole walls to undergo spalling, or buffer blocks may be able to move around within these gaps [7].

In Korea, an improved geological disposal system was developed as described in the Korea Atomic Energy Research Institute (KAERI) Reference Disposal System Plus concept of 2020; nevertheless, this system still does not consider the impact of gaps in an EBS [8], which can influence the performance of different EBS components [4,9]. Notably, there is a need to analyze how the gaps affect the temperature of bentonite buffer materials. Many countries set the upper limit for buffer temperature exposure at 100 °C, based on the KBS-3 concept in crystalline rocks [3,10]. Such a restriction is necessary because bentonite undergoes mineralogical deterioration when exposed to high temperatures for extended periods, which results in the deterioration of its buffering properties (e.g., swelling capacity) that are required for proper EBS functioning [11]. However, several studies have investigated bentonite properties above 100 °C to assess the effects of increasing the upper temperature limit of buffer material [11,12]. Nevertheless, in contrast to a significant amount of research focusing on EBS components, very few studies have investigated the gaps that are shaped

* Corresponding author.
E-mail address: syoon@kaeri.re.kr (S. Yoon).

https://doi.org/10.1016/j.net.2023.07.032
Received 7 March 2023; Received in revised form 23 June 2023; Accepted 24 July 2023
Available online 26 July 2023

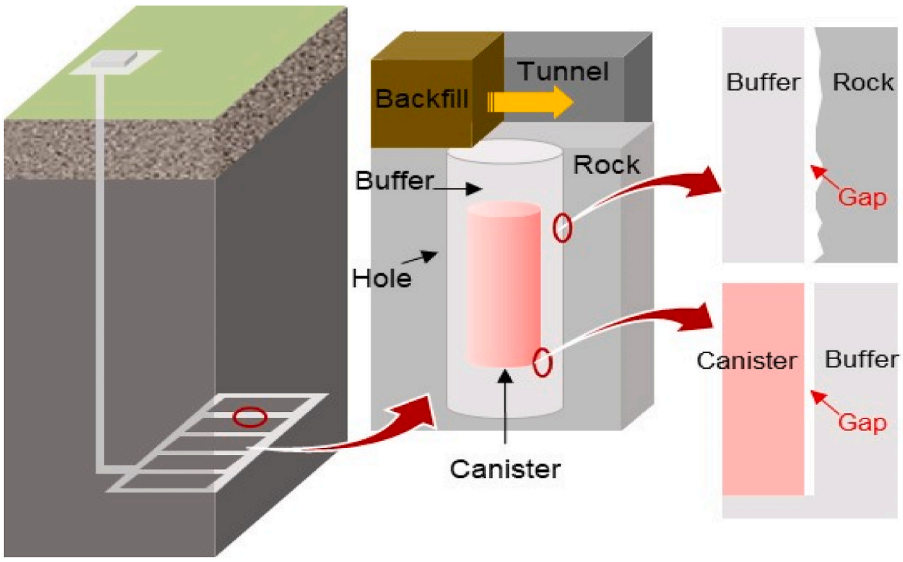

Fig. 1. Gap spaces in an engineered barrier system [4].

Table 1
Basic properties of bentonite powder [15].

Property	Gyeongju bentonite
Water content (%)	11~12%
Swelling index (mL/2 g)	6.5
Specific gravity	2.71
Specific surface area (m^2/g)	61.5
Cation exchange capacity (meq/100 g)	64.7
Plastic limit (%)	28.4
Liquid limit (%)	146.7

between such components.

Here, our objective was to investigate empirically how bentonite temperature varies with changes in the gaps that occur between EBS components. This involved the installation of bentonite blocks within a steel canister and examining the temperature trends as this buffer material was heated from room temperature to 100 °C in setups with and without gaps.

2. Methods

2.1. Materials and test equipment

Ca-type bentonite powder in which Ca^{2+} is the dominant exchangeable cation was obtained from Clariant Korea Ltd. (Seoul, Korea). This powder is generally compressed into block shapes for use as buffer material in an EBS [13,14], and Table 1 lists the basic properties of identical bentonite powder used in this study [15]. Mineral and the chemical components were characterized via X-ray diffraction [16] and X-ray fluorescence [17] analyses, respectively. The main mineral components were montmorillonite (62%), ablite (21%), and quartz (5%). Ca-type bentonite has a montmorillonite crystal nucleus with abundant Ca^{2+} cations [18], and its main chemical components are SiO_2 and Al_2O_3; the amount of CaO (5.72%) in the powder was 5–6 times higher than that of Na_2O (1.06%) [19]. The cation exchange capacity (CEC) of the bentonite was determined to be 64.7 meq/100 g through the barium chloride method [20]. The specific area of the bentonite was 61–62 m^2/g. In terms of basic geotechnical properties, the bentonite powder used in this study was classified as having high plasticity (CH) [19] by using the unified soil classification system [21]. The thermal conductivity and specific heat of bentonite powder are 0.092–0.099 W/(m·K) and 0.873–0.877 (kJ/kg·K) when the dry density of the bentonite is 0.98 g/cm^3 and the bentonite is in a dry state [19].

Table 2
Experimental cases.

Scenario	Components	Note
Scenario 1	Only air	
Scenario 2	Air + bentonite	2 mm air gap between cell and bentonite
Scenario 3	Bentonite	No gap

2.2. Experimental setup

Bentonite powder was compacted into a block with a steel mold and hydraulic press. The initial dry density, water content, and thermal conductivity of the compacted bentonite block were 1.61 g/cm^3, 11–12%, and 0.85 W(m·K), respectively. A temperature sensor (EE310; E + E Elektronik, Engerwitzdorf, Austria) with an accuracy of ± 0.2 °C was inserted into a groove that was dug into the bentonite sample. Next, a cylindrical cell (internal diameter: 50 mm; height: 72 mm) was manufactured from 304 stainless steel. An external heating jacket was used to adjust the temperature around the cell. Temperatures of the bentonite sample and cell surface were measured with and logged into a data logging system. As described in Table 2 and Fig. 2, experiments were

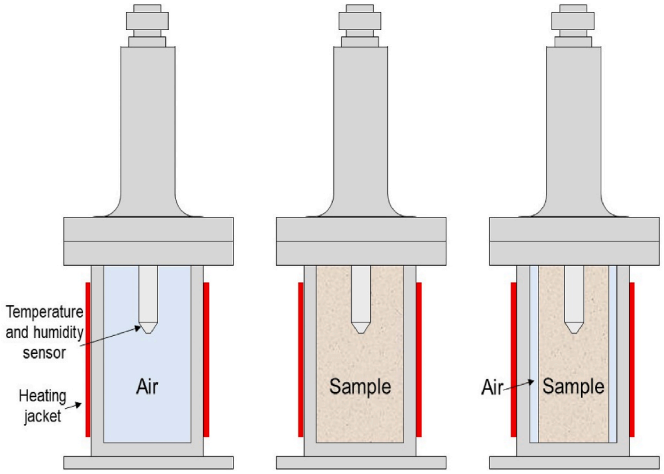

Fig. 2. Diagram of experimental cases.

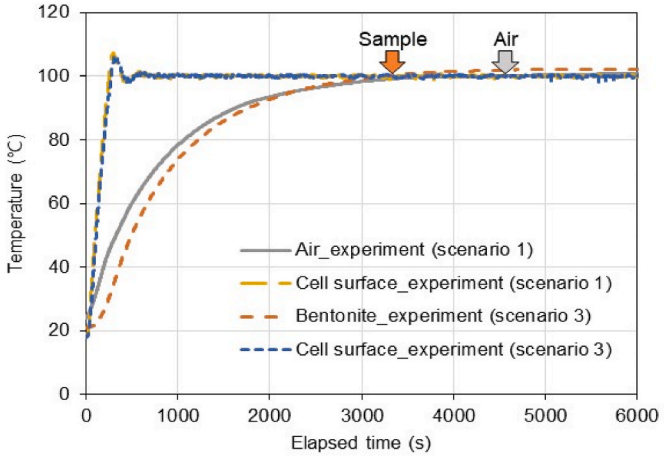

Fig. 3. Experimental results for the temperature variation of the air, compacted bentonite, and cell surface.

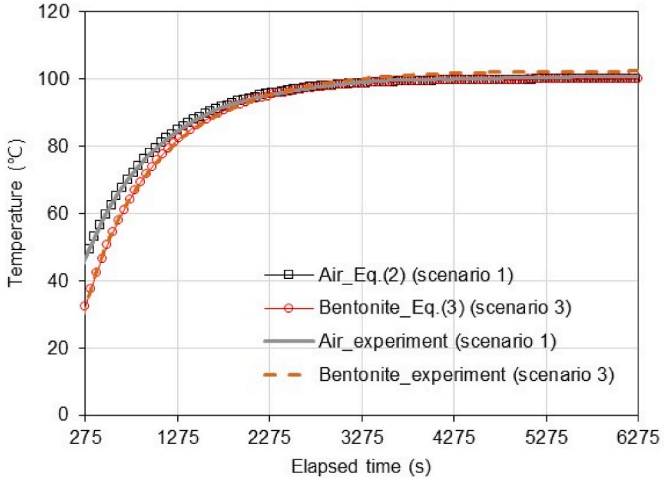

Fig. 4. Comparison of experimental results and analytical solution.

performed for three scenarios to analyze how the temperature of bentonite change when the temperature of the overall experimental system is increased from room temperature to 100 °C. Once the temperature of the cell reached 100 °C, the heating jacket could maintain this as a constant temperature inside the inner cell, compensating for any temperature loss to the external environment. In scenario 1, the stainless steel cell contained only air (no bentonite); in scenario 2, a bentonite sample 46 mm in diameter was placed within the cell (mostly bentonite and air); in scenario 3, the 50 mm diameter cell was completely filled with a 50 mm diameter bentonite sample (bentonite only).

3. Results and discussion

3.1. Validation of experimental system

To verify the reliability of our experimental results, the temperature of the air (scenario 1) and the compacted bentonite (scenario 3) in the stainless steel cells were measured. Fig. 3 shows the experimental results regarding the temperature variation of the air, bentonite, and heater surface. The temperature variation of a heat transfer medium with respect to time can be derived using Newton's law of cooling [22,23], using the formula in Eq. (1) below:

$$\frac{dT}{dt} = -k(T - T_A) \tag{1}$$

where t is the time (min), k is a constant, T is the sensor temperature inside the cell (°C), and T_A is the cell surface temperature (°C). When the cell surface first reached 100 °C, time was established as $t = 0$. Eq. (1) was applied using the sensor temperature inside the cell when $t = 10$ (min), when the cell surface temperature reached convergence. Consequently, for a cell in which the interior is filled with only air, Eq. (1) can be expressed as follows:

$$T_{air}(t) = -54.57e^{-0.075t} + 100 \tag{2}$$

When the inside of the cell is filled with a compacted bentonite sample, as in scenario 3, Eq. (1) can be expressed as follows:

$$T_{sample}(t) = -67.6e^{-0.079t} + 100 \tag{3}$$

Because the interior of the cell is a confined space, the pressure in the cell increases along with an increase in temperature; as a result, heat conduction occurs faster with the active movement of air molecules [24,25], and the measured temperature may be higher than that of the model. Nevertheless, the experimental results obtained using Eq. (2) and Eq. (3) showed very similar trends when the analytical formula for each experimental condition was compared with that after the cell surface first reached 100 °C. In our assessment of the accuracy of the experimental environment, including the process of convergence of the cell surface temperature to 100 °C (Fig. 4), the experimental results followed Newton's law of cooling with relative accuracy. Therefore, it can be assumed that our experimental system accurately reflected the temperature variation of compacted bentonite (with or without gap effects).

3.2. Experimental results

Experiments were performed for the three scenarios described in Table 2. The rate at which heat from the heating jacket was transferred to the cell varied, depending on the initial temperature of the cell surface. For a more accurate analysis, the experiments were performed by initially heating all cell surfaces to 100 °C and then measuring and comparing the times required for the temperature readings of the sensors inside the cells to reach 100 °C.

In scenario 1 (only air in the cell), the initial temperature of the cell surface at the beginning of the experiment was 18.80 °C and that of the cell interior was 23.90 °C. Upon activation of the heating jacket, the cell surface temperature increased sharply to 100 °C, rose to approximately 107 °C, then started to decrease until settling at 100 °C. Overall, 255 s (4.25 min) were required for the cell surface temperature to reach 100 °C. According to the internal sensor, 4554 s (75.90 min) was required to reach an internal temperature of 100 °C. In other words, 4299 s (71.65 min) elapsed before the internal temperature matched that of the cell surface.

Scenario 2 included both an air layer and bentonite material inside the stainless steel cell. At the onset of the experiment, the surface and interior cell temperatures were 18.90 °C and 22.46 °C, respectively. It took 267 s (4.45 min) for the surface temperature to rise to 100 °C following activation of the heating jacket. Thereafter, the surface temperature continued to increase to approximately 106 °C, after which it fluctuated until finally reaching a plateau at 100 °C. A total of 4467 s (74.45 min) elapsed before the temperature reading of the sensor inside the cell reached 100 °C. This translated to a time of 4200 s (70.00 min) for the internal temperature to match the 100 °C reached on the cell surface.

For scenario 3 (with a 50 mm diameter compacted bentonite sample filling the cell), the cell surface and interior temperatures at the beginning of the experiment were 18 °C and 21.02 °C, respectively. This represented a starting internal temperature 2.88 °C lower than that for Case 1. Following activation of the heating jacket, it took 275 s (4.58 min) for the cell surface to reach 100 °C. The cell surface temperature increased to approximately 106 °C, then fluctuated until plateauing at

Table 3
Time to reach 100 °C inside the cell in each experimental case.

	Air (case 1)	Bentonite (case 2)	Bentonite (case 3)
Initial temperature of cell interior (°C)	23.9	22.46	21.02
Initial temperature of the cell surface (°C)	18.8	18.9	18
Time at which the cell surface first reached 100 °C (s)	255	267	275
Time for the temperature inside the cell to reach 100 °C (s)	4554	4467	3257
Time for the temperature inside the cell to reach 100 °C after the cell surface first reached 100 °C (s)	4299	4200	2982

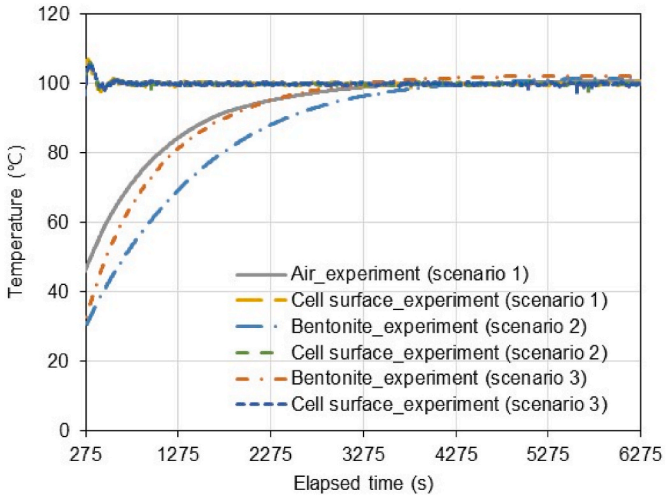

Fig. 5. Summary of experimental results.

100 °C. A total of 3256 s (54.27 min) elapsed for the temperature inside the cell to reach 100 °C, which represented an elapsed time of 2982 s (49.70 min) to match the cell surface temperature.

In comparing the results from scenario 1 and 3, the cell filled with bentonite reached an internal temperature of 100 °C that matched the external 100 °C approximately 1317 s (22.00 min) faster than the empty cell did. This discrepancy can be explained by the difference in thermal conductivity between the media within the two cells. Because the thermal conductivity of bentonite is significantly higher than that of air, heat was transferred to the center of the cell faster via the buffer sample. In comparing the results from scenario 1 and 3, the empty cell of scenario 2 took 99 s (1.65 min) less for its internal temperature to reach 100 °C after its surface had been heated to the same temperature. The bentonite diameter was 4 mm smaller than the inner diameter of the surrounding cell. Although the sample occupied most of the space within the cell, the time taken for the internal sensor reading to reach 100 °C was similar to that of the cell containing only air. Considering the small scale of this experiment, the loss in heat transfer efficiency of actual deep disposal sites can be expected to be substantial if gaps are present in the buffer layers. This emphasizes a need to fill any rock–buffer gaps with suitable material [4,5]. Furthermore, as gaps also interfered with heat transfer from our stainless steel cell to the compacted bentonite, it can be advantageous to retain buffer–cannister gaps in practice to lower the peak temperature of the buffer. Lee et al. [9] reported similar results based on numerical simulations. It might be thought that there is just air between canister and buffer material in this reason. Table 3 and Fig. 5 summarize our findings across the three different experimental scenarios.

4. Conclusion

This study conducted laboratory experiments to analyze how air spaces between the EBS components (which are installed for the deep disposal of high-level waste) influence temperature changes in the system.

First, to verify the consistency of the experimental system, we conducted temperature measurements on an empty stainless steel cell and one completely filled with bentonite. Overall, the measured values were mostly consistent with Newton's law for the cooling model. The subsequent experiments also included a cell with a 2 mm air gap between its inner wall and a bentonite sample. The cells in the three scenarios (empty, partially filled, or filled completely with bentonite) did not start at the same initial temperature, and each cell required different lengths of time for the cell surface to reach 100 °C. Once the cell surfaces reached 100 °C, we measured the time required for the inside of each cell to reach the same temperature. The cell lacking gaps between the bentonite sample and its surrounding wall reached 100 °C within the shortest length of time. Compared to this cell, the one with a 2 mm air gap between the bentonite and the cell wall took 1.3 times longer for the core to reach 100 °C. This can be ascribed to poor heat transfer, given that the thermal conductivity of air is substantially lower than that of bentonite.

Our findings confirmed that the time that it takes buffer materials in an EBS to reach their maximum temperature can be influenced by the presence of air gaps between the different components. In particular, rock–buffer spaces should be filled to ensure the rapid dissipation of heat from the buffer material to its surroundings. Furthermore, given that the diameter of our bentonite sample was rather small at 50 mm, it will be necessary to establish an experimental system at a larger scale that also considers the effect of natural water infiltration on the bentonite saturation process.

Declaration of competing interest

We have no conflict of interest to declare.

Acknowledgements

This research was supported by the Nuclear Resdearch and Development Program of the National Research Foundation of Korea (2021M2E3A2041351) and the Institute for Korea Spent Nuclear Fuel and the National Research Foundation of Korea (2021M2E1A1085193).

References

[1] W.Z. Chen, Y.S. Ma, H.D. Yu, F.F. Li, X.L. Li, X. Sillen, Effects of temperature and thermally-induced microstructure change on hydraulic conductivity of Boom Clay, J. Rock Mech. Geotech. Eng. 9 (2017) 383–395.
[2] W.J. Cho, Radioactive Waste Disposal, KAERI, 2017. KAERI/GP-495/2017.
[3] S.K.B. Posiva, Safety Functions, Performance Targets and Technical Design Requirements for a KBS-3V Repository, Posiva SKB, 2017. Report 02.
[4] S. Yoon, M.J. Kim, S. Chang, G.J. Lee, Evaluation on the buffer temperature by thermal conductivity of gap-filling material in a high-level radioactive waste repository, Nucl. Technol. Eng. 54 (2022) 4005–4012.
[5] J.O. Lee, Y.C. Choi, H.J. Choi, R&D Status on Gap-Filling Materials for the Buffer and Backfill of a HLW Repository, KAERI, 2013. KAERI/AR-1005/2013.
[6] P. Marjavaara, H. Kivikoski, Filling the Gap between Buffer and Rock in the Deposition Hole, Posiva Oy, 2011. Working Report 2011-33.
[7] M. Juvankoski, Buffer Design 2012, Posiva Oy, 2013, pp. 2012–2014. Posiva.
[8] J. Lee, H. Kim, I. Kim, H. Choi, D. Cho, Analyses on thermal stability and structural integrity of the improved disposal systems for spent nuclear fuels in Korea, J. Nucl. Fuel Cycle Waste Technol. 18 (S) (2020) 21–36.
[9] J.O. Lee, H.J. Choi, G.Y. Kim, D.K. Cho, Numerical analysis of the effect of gap-filling options on the maximum peak temperature of a buffer in a HLW repository, Prog. Nucl. Energy 111 (2019) 138–149.
[10] J. Rutqvist, Thermal management associated with geologic disposal of large spent nuclear fuel canisters in tunnels with thermally engineered backfill, Tunn. Undergr. Space Technol. 102 (2020), 103454.

[11] T.J. Park, D. Seoung, Thermal behavior of groundwater-saturated Korean buffer under the elevated temperature conditions: in-situ synchrotron X-ray powder diffraction study for the montmorillonite in Korean bentonite, Nucl. Eng. Technol. 53 (2021) 1511–1518.
[12] L. Zhen, J. Rutqvist, J.T. Birkholzer, H.H. Liu, On the impact of temperatures up to 200 °C in clay repositories with bentonite engineer barrier systems: a study with coupled thermal, hydrological, chemical, and mechanical modeling, Eng. Geol. 197 (2015) 278–295.
[13] SKB, Manufacturing of Large Scale Buffer Blocks, SKB, 2020. R-19-28.
[14] J.S. Kim, S. Yoon, W.J. Cho, Y.C. Choi, G.Y. Kim, A study on the manufacturing characteristics and field applicability of engineering-scale bentonite buffer block in a high-level nuclear waste repository, J. Nucl. Fuel Cycle Waste Technol. 16 (2018) 123–136.
[15] S. Yoon, S. Chang, D. Park, Investigation of soil-water characteristic curve for compacted bentonite considering dry density, Prog. Nucl. Energy 151 (2022), 104318.
[16] H. Khan, A.S. Yerramilli, A. D'Oliveira, T.L. Alford, D.C. Boffito, G.S. Patience, Experimental methods in chemical engineering: X-ray diffraction spectroscopy—XRD, Can. J. Chem. Eng. 98 (6) (2020) 1255–1266.
[17] C.Y. Major, XRF method XRF analysis of rocks and minerals for major and trace elements on a single low dilution Li-tetraborate fused bead, Adv. X Ray Anal. 41 (1999) 843–867.
[18] Y. Qin, D. Xu, B. Lalit, Effect of bentonite content and hydration time on mechanical properties of sand-bentonite mixture, Appl. Sci. 11 (2021), 12001.
[19] G.J. Lee, S. Yoon, T. Kim, S. Chang, Investigation of the various properties of several candidate additives as buffer materials, Nucl. Eng. Technol. 55 (3) (2023) 1191–1198.
[20] W.H. Hendershot, M. Duquette, A simple barium chloride method for determining cation exchange capacity and exchangeable cations, Soil Sci. Am. J. 50 (1986) 605–608.
[21] B.M. Das, Principle of Geotechnical Engineering, sixth ed., Nelson, Scarborough, 2006.
[22] I. Newton, The Principia, (1687), Translated by A. Motte, Prometheus Books, Buffalo, New York, 1972, pp. 187–188.
[23] S. Maruyama, S. Moriya, Newton's law of cooling: follow up and exploration, Int. J. Heat Mass Tran. 164 (2021), 120544.
[24] S. Dahariya, A.R. Betz, Theoretical and experimental analysis of increasing pressure during pool-boiling, in: Proceedings of the ASME 2018 16th International Conference on Nanochannels, Microchannels, and Minichannels, Dubrovnik, Croatia, June 10-13, 2018.
[25] J. Cui, C. Lei, Z. Xing, C. Li, S. Ma, Predictions of the mechanical properties and microstructure evolution of high strength steel in hot stamping, J. Mater. Eng. Perform. 21 (2012) 2244–2254.